

Accepted Manuscript

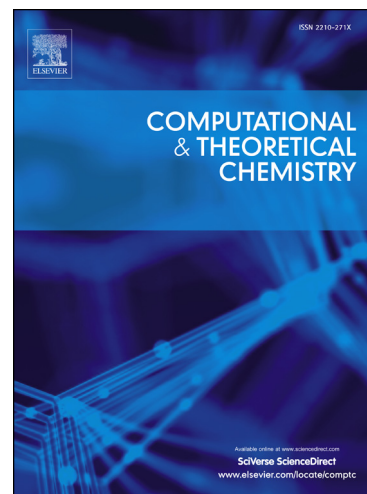
Heterocyclic azo dyes for dye sensitized solar cells: A Quantum chemical study

Asif Mahmood, Mudassir Hussain Tahir, Ahmad Irfan, Abdullah G. Al-Sehemi,
M.S. Al-Assiri

PII: S2210-271X(15)00217-0
DOI: <http://dx.doi.org/10.1016/j.comptc.2015.05.020>
Reference: COMPTC 1827

To appear in: *Computational & Theoretical Chemistry*

Received Date: 7 September 2014
Revised Date: 22 May 2015
Accepted Date: 24 May 2015



Please cite this article as: A. Mahmood, M.H. Tahir, A. Irfan, A.G. Al-Sehemi, M.S. Al-Assiri, Heterocyclic azo dyes for dye sensitized solar cells: A Quantum chemical study, *Computational & Theoretical Chemistry* (2015), doi: <http://dx.doi.org/10.1016/j.comptc.2015.05.020>

This is a PDF file of an unedited manuscript that has been accepted for publication. As a service to our customers we are providing this early version of the manuscript. The manuscript will undergo copyediting, typesetting, and review of the resulting proof before it is published in its final form. Please note that during the production process errors may be discovered which could affect the content, and all legal disclaimers that apply to the journal pertain.

Heterocyclic azo dyes for dye sensitized solar cells: A Quantum chemical study

Asif Mahmood^{a*}, Mudassir Hussain Tahir^a, Ahmad Irfan^{b,c}, Abdullah G. Al-Sehemi^{b,c}, M.S. Al-Assiri^{d,e}

^aDepartment of Chemistry, University of Sargodha, Sargodha 40100, Pakistan

^bDepartment of Chemistry, Faculty of Science, King Khalid University, Abha 61413, P.O. Box 9004, Saudi Arabia

^c Research Center for Advanced Materials Science, King Khalid University, Abha 61413, P.O. Box 9004, Saudi Arabia

^dDepartment of Physics, Faculty of Sciences and Arts, Najran University, P.O. Box 1988, Najran 11001, Saudi Arabia

^e Promising Centre for Sensors and Electronic Devices (PCSED), Najran University, P.O. Box 1988, Najran 11001, Saudi Arabia

*E-mail: asifmahmood023@gmail.com

Abstract

This study was carried out to design heterocyclic azo dyes for dye sensitized solar cells. Quantum chemical calculations were performed to determine the open-circuit photovoltage (V_{OC}), and to quantify the parameters such as the light harvesting efficiency, the electron injection efficiency associated with the short-circuit photocurrent density (J_{SC}). All the dyes showed absorbance in visible region (502-521 nm) with high oscillator strength (f) (0.473-0.961) and light harvesting efficiency (LHE) (0.663-0.891). After binding to titanium oxide, all dye showed slightly red-shifted absorption (521-527 nm) with improved oscillator strength (f) (0.573-0.991) and light harvesting efficiency (LHE) (0.733-0.898). There is high probability that these dyes will show larger J_{SC} due to high driving force for electron injection. These dyes also showed high V_{OC} (1.037-1.128 eV). These results indicate that heterocyclic azo dyes will show better light to power conversion efficiency in DSSCs due to high J_{SC} and V_{OC} . These theoretical criteria would be useful to design and fast screen other organic dyes, specifically for chemically similar dyes.

Keywords: Organic dyes, Dye sensitized solar cells, heterocyclic azo dyes, Density functional theory, efficiency.

1. Introduction

Dye sensitized solar cells (DSSCs) have gotten increasing attention as potential alternatives due to their efficient conversion of solar energy to electricity at a low cost [1-4]. In past two decades

different photosensitizers have been designed and applied to DSSCs [5, 6]. Ruthenium complexes showed overall conversion efficiency over 11% [7]. But their application is limited due to high cost, limited reserves of ruthenium and environmental risk. Organic sensitizers, e.g. triphenylamine derivatives [8-10], azo dyes [11], hydrazones[12] etc. have been extensively studied due to their unique advantages, such as low-cost, environmental friendly and tunable properties[13-15].

Extensive work has done for the designing of high efficiency metal-free organic dyes for DSSCs. The novel designed dyes with the donor-bridge-acceptor (D- π -A) system can usually achieve an efficient photovoltaic performance. Dyes play an important role in gaining higher solar-to-electricity conversion efficiency because the performance of DSSCs strongly depends on the following factors which are the criteria for a good dye sensitizer: (i) Wide absorption wavelength in visible to near infrared (IR) region; (ii) Easy electron injection from the excited state of the dyes to the conduction band of TiO_2 and (iii) Good electron transfer from the donor to acceptor. All these factors are closely associated with the ground and excited electronic states of the dye sensitizer.

The bathochromic shift of the absorption maxima is one of the most important challenges to improve the DSSCs performance. Snaith proposed that with the loss-in-potential of the present state-of-the-art DSSCs (0.75 eV), a maximum efficiency of 13.4% is achievable employing a sensitizer with an absorption onset at 840 nm [16]. Reducing the loss-in-potential to that of the least “lossy” DSSC reported to date (0.66 eV) results in a maximum efficiency of 15.1% with an absorption onset at 920 nm [17]. The first issue could be fulfilled by the introduction of electron-donating groups onto the donors, introduction of electron-rich and electron-withdrawing groups onto the π -bridges, or incorporation of a longer conjugated segment in the push-pull system. Therefore, choosing a suitable donor group in the D- π -A system is very critical to balance between photo-voltage, driving forces and spectral response for the preparation of high efficiency dyes [18].

But every time enhancing the efficiency of the dyes by simple expansion of the π -conjugated system through increasing the number of electron-rich segments (such as thiophene) was not an effective strategy, because the halogen bonding between iodine and some electron-rich segments

of the dye molecules could cause a larger charge recombination rate at the titania/electrolyte interface.

Computational chemistry has emerged in the past 20 years as one of the most powerful tools for generating highly accurate models of molecular systems and materials. The development of dye sensitized solar cells has been accompanied by computational chemistry studies that helped to rationalize the relationship between the chemical structure and device performance. In particular, electronic and optical absorption properties of dye molecules, both isolated and adsorbed on the semiconductor (TiO_2) surfaces, have been extensively studied using density-functional theory (DFT) and time-dependent DFT, in order to help identify dyes with broad adsorption spectra and favorable electron transfer from the photoexcited dye to the semiconductor [19].

Heterocyclic azo dyes have been widely investigated mostly due to their application for coloring textiles and plastics. Thiophene, pyrrole and azoles bearing azo dyes have been used for electronic applications such as optical switching, second harmonic generation and organic sensitized solar cells [20, 21]. Over the past decade, there has been a number of articles and patents detailing the use of azo dyes as sensors [22]. Azo dyes combine their optical and electronic properties with good chemical stability and solution processability [23], which makes them interesting for DSSC applications. Nevertheless, there is a small number of reports on DSSCs with azo dyes as sensitizers [21].

With the aim to shed light on the electro-optical and charge transport properties in azo sensitizers, we have performed this study. In the best of our knowledge, no detailed computational study has been performed about the highest occupied molecular orbitals (HOMOs), lowest unoccupied molecular orbitals (LUMOs), absorption wavelengths, electron injection and light harvesting efficiency (LHE) of our adopted azo dyes and dyes@ TiO_2 cluster. Density functional theory (DFT) and time-dependent DFT (TD-DFT) methods are used to calculate the above mentioned properties of interests. Open-circuit photovoltage (V_{oc}) and key parameters controlling short-circuit current density (J_{sc}) were also calculated. The effect of dye adsorption on the TiO_2 cluster has been studied with respect to the distribution patterns of the frontier molecular orbitals, oscillator strengths and excitation energies.

2. Computational details

All the calculations were performed with the Gaussian 09 program package [24]. The structure optimization of the ground state of the dyes in gas phase have performed by using B3LYP functional[25] and 6-31+G* basis set [26]. A tight SCF convergence criteria (10^{-8} a.u.) and integration grid of 10^{-8} were used for all calculations. Frequency calculations have been performed on the optimized geometry to verify the nature of the computed geometries. The lack of imaginary values in the wave numbers calculations indicated the successful geometry optimization.

For a reasonable computational effort, the state of the art DFT/TDDFT computational methodologies provide reasonable results and reproduce well the optical properties of various organic dyes [27-30]. We first examined the effect of the functionals and basis set on λ_{\max} of reference dye. Table 1 presents a comparison between simulated and experimental λ_{\max} of reference dye[31]. Table 1 depicts that CAM-B3LYP/6-31+G* is best methodology that produced result comparable to experimental value. This methodology is used to simulate the UV/Vis spectra of designed dyes.

Coulomb-attenuating method CAM-B3LYP functional[32]taking long-range correction into account, which has been proven to be appropriate for charge transfer (CT) type excitations[33-35], was chosen to calculate the excitation energies and the oscillator strengths. Solvent effect (acetone) was undertaken using conductor-like polarizable continuum model (CPCM) with UAHF radii[36]. $\text{Ti}_5\text{O}_{20}\text{H}_{22}$ cluster was optimized in gas phase using B3LYP functional and 6-31+G* basis set for non-metal atoms while LANL2DZ basis set [37-39] for Ti atom. Dye@ $\text{Ti}_5\text{O}_{20}\text{H}_{22}$ systems were also optimized using same approach. CAM-B3LYP functional and 6-31+G* basis set for non-metal atoms while LANL2DZ basis set for Ti atom were used to calculate the UV/vis spectra of Dye@ $\text{Ti}_5\text{O}_{20}\text{H}_{22}$ systems.

3. Results and discussion

In this study, we presented the results of theoretical designing of efficient sensitizers for dye sensitized solar cells. Structures of dyes heterocyclic azo are given in Figure 2. DFT and TDDFT calculations were performed to study the dyes. Key parameters: (i) open-circuit photovoltage (V_{oc}); (ii) light harvesting efficiency (LHE); (iii) injection driving force (ΔG^{inject}) were calculated.

3.1. Energy level alignment

Suitable energy levels and locations of the HOMOs and LUMOs of the dye sensitizer are required to match the iodine/iodide redox potential and the conduction band edge level of the TiO₂ semiconductor [40]. The energy level diagram of the HOMOs and LUMOs of the dyes, E_{cb} of TiO₂ and redox potential energy of the electrolyte are presented in Figure 3. For all the dyes considered here, the simulated LUMOs lie above the TiO₂ conduction band edge (4.00 eV in vacuum) [41], providing the thermodynamic driving force for favorable electron injection from the excited state dye to the TiO₂ conduction band edge. Meanwhile the HOMOs of all dyes lie below the iodide redox potential (4.80 eV in vacuum) [42], leading to a fast dye regeneration and avoiding the geminate charge recombination between oxidized dye molecules and photo-injected electrons in the nanocrystalline titania film.

3.2. UV-Vis spectra of dyes

To gain insight into the excited states responsible for intense absorption spectra of sensitizers, TD-DFT calculations were performed at the CAM-B3LYP/6-31+G* level. In the TD-DFT calculations of absorption spectra, the 20 lowest singlet-singlet transitions were taken into account.

The computed maximum absorption wavelengths (λ_{max}), absorption energy, oscillator strengths (f) and nature of the transitions are summarized in Table 2. All the dyes showed absorption in visible region (502-521 nm). Absorbance in visible region is required for high efficiency. Oscillator strengths were also high (0.473-0.961). Another factor related to efficiency of DSSC is the performance of the dyes to response the incident light. Values of light harvesting efficiency (LHE) have to be as high as possible to maximize the photocurrent response. The LHE can be expressed as [43]:

$$LHE = 1 - 10^{-f} \Rightarrow (1)$$

Where f is the oscillator strength. Values of LHE are given in Table 2. LHE values were high (0.663-0.891).

3.3 Adsorption of dyes on TiO₂ surface

A correct prediction of the adsorption geometry of the dye is an essential prerequisite for the theoretical description of the interface electronic structure and the charge transfer characteristics. The effect of adsorption on the electronic structure, especially the positions of the dye's LUMO and the conduction band (CB) of TiO_2 , are of the greatest relevance for the physics of DSSC devices, because the energies of these levels affect injection rates (and therefore the short-circuit current J_{SC}) and the open-circuit voltage V_{OC} , and thus the efficiency of the solar cell. Most of the theoretical studies of dyes' adsorption have considered adsorption on TiO_2 surfaces, especially the most stable anatase (101) and rutile (110) surface.

Nature of excited states of semiconductor/dye interface controls the electron injection rate from dye to semiconductor. Hence, the computational modeling of semiconductor/dye interface is considered to be a very useful tool to optimized DSSCs. In this regard, simulations of the electronic and optical properties of TiO_2 nanoparticles and the dye excited states were performed.

3.3.1 Adopted model for TiO_2 film

Semiconductor is one of the main components in the DSSCs and nano structured TiO_2 has frequently been used in the most efficient DSSC systems. TiO_2 has three major crystalline structures; rutile, anatase and brookite. However, the electrodes in photovoltaic cells are often based on anatase and the (101) surface of anatase is thermodynamically most stable surface[3, 44]. $\text{Ti}_5\text{O}_{20}\text{H}_{22}$ (101) model from crystal structures is adopted as surface of TiO_2 film in the current work.

The TiO_2 surfaces were generated from the optimized bulk geometry exposing the most thermodynamically stable (101) surface of anatase. Our TiO_2 model is not cluster model, which is cut out from relaxed surface slab. These Ti atoms can be divided into two types: One is five-coordinated and another is six-coordinated. The five-coordinated Ti atoms are located at anatase (101) surface, which used for adsorption site. In addition, the six-coordinated Ti atoms cut out from the TiO_2 crystal bulk. And hydrogen saturators were used on oxygen atoms, and this method not only maintains bond-orientation in crystal, but also avoids the chaos of charge and multiplicity in the whole system. This model is small enough that the relatively large basis set (6-

31+G*) can be adopted in calculation. From several adsorption configurations, bidentate chelating adsorption mode is used which is energetically more favorable [3].

3.3.2 Electronic and Optical Properties of the Dye@TiO₂ System

It is found that electronic and optical properties of dyes showed significant changes when absorbed to TiO₂, might be due to interaction between the dyes and the semiconductor. Therefore, we have also simulated the UV/Vis absorption spectra of the dyes after binding to Ti₅O₂₀H₂₂ cluster at the same level of theory for the free dyes except that the LANL2DZ basis set was used for Ti atom. The results from these investigations are listed in Table 3. Average calculated distances between the carboxylic oxygen atoms and the TiO₂ surface (O–Ti bond) was 2.0–2.1 Å. This shorter distance indicates probably stronger electronic coupling between dyes and semiconductor. We found that after binding to TiO₂, dyes showed red-shift in the maximum absorption wavelengths. Red-shift of absorption spectra of dye after binding TiO₂ can be explain on the basis of interactions between electron acceptor group of dye (–COOH) and the 3d orbitals of the Ti atom, resulting an overall decrease in the LUMO energies as compare with the isolated dyes. Oscillating strength (*f*) was improved due to the interaction between the dyes and the semiconductor comparing with the free dyes. In addition, after binding to the semiconductor, the LHE of the dyes showed an increase. HOMOs and LUMOs of dyes@TiO₂ are given in Figure 4.

3.4. Performance of DSSCs based on dyes

The overall efficiency of the DSSC can be calculated from the integral of short-circuit photocurrent density (*J_{sc}*), open circuit potential (*V_{oc}*), the fill factor (*ff*) and the intensity of light (*I_s*), expressed by

$$\eta = \frac{V_{oc} J_{sc} FF}{I_s} \times 100\% \Rightarrow (2)$$

3.4.1 Factors influencing *J_{sc}*

The *J_{sc}* in DSSCs is determined by the following equation:

$$J_{sc} = \int_{\lambda} LHE(\lambda) \Phi_{inject.} \eta_{collect.} d\lambda \Rightarrow (3)$$

where $LHE(\lambda)$ is the light harvesting efficiency at a given wavelength, $\Phi_{inject.}$ is the electron injection efficiency, and $\eta_{collect.}$ is the charge collection efficiency. For the same DSSCs with only different dyes, just as for the organic dyes under study, it is reasonable to assume that the $\eta_{collect.}$ is a constant. As a result, the enhancement of J_{SC} should focus on improving the LHE and $\Phi_{inject.}$

As discussed above, if the charge collection efficiency ($\eta_{collect.}$) could be considered as a constant for the same cell architecture, LHE and $\Phi_{inject.}$ are the two main factors influencing J_{SC} . According to eqn (3), in order to obtain a high J_{SC} , the efficient organic dyes used in DSSCs should have a large LHE. The LHE of dyes was high.

Another way to enhance J_{SC} is to improve $\Phi_{inject.}$ which is related to the driving force (ΔG^{inject}) of the electron injection from the photoinduced excited states of organic dyes to the TiO_2 surface. In general, larger ΔG^{inject} leads to larger $\Phi_{inject.}$

Computation of electron injection rate is very useful to study photovoltaic data. Following equation is used to calculate free energy change (in eV) for the electron injection:

$$\Delta G^{inject} = E_{OX}^{dye*} - E_{CB}^{TiO_2} \Rightarrow (4)$$

where E_{OX}^{dye*} is the oxidation potential of the dye in the excited state, $E_{CB}^{TiO_2}$ is the reduction potential of the conduction band of the TiO_2 ($E_{CB}^{TiO_2} = 4.0\text{eV}$). E_{OX}^{dye*} can be estimated by [45]:

$$E_{OX}^{dye*} = E_{OX}^{dye} - E_{00} \Rightarrow (5)$$

where E_{OX}^{dye} is the oxidation potential energy of the dye in the ground state, while E_{00} is an electronic vertical transition energy corresponding to the λ_{max} . E_{OX}^{dye} can be estimated as negative E_{HOMO} [46]. By using this scheme, we calculated ΔG^{inject} , as well as E_{OX}^{dye} and E_{OX}^{dye*} for dyes and the results are listed in Table 4. We found that all the calculated ΔG^{inject} were negative, which means that the dye excited state lies above the TiO_2 conduction band edge, favoring the injection of the electron from the excited state dye to the TiO_2 conduction band edge. Dyes would show

higher J_{SC} due superior LHE and $\Delta G^{inject}(\Phi_{inject.})$. Moreover, the calculated ΔG^{inject} of all the four studied dyes 1-4 have been observed -0.103, -0.191, -0.237 and -0.136 revealing that dye 3 might have superior light to power conversion efficiency than other counterparts.

3.4.2. Open-circuit photovoltage (V_{OC})

The V_{OC} is obtained only by experiment, the relationship among these quantities and the electronic structure of dye is still unknown. The analytical relationship between V_{OC} and E_{LUMO} may exist. According to the sensitized mechanism (electron injected from the excited dyes to the semiconductor conduction band) and single electron and single state approximation, there is an energy relationship [47]:

$$eV_{OC} = E_{LUMO} - E_{CB} \Rightarrow (6)$$

where E_{CB} is the energy of the semiconductor's conduction band edge. It is known that the higher the E_{LUMO} , the larger the V_{OC} . High values of LHE, ΔG^{inject} and eV_{OC} indicate that all dyes would show high efficiency in dye sensitized solar cell.

4. Conclusions

Open-circuit photovoltage (V_{OC}), factors influencing the short-circuit current density (J_{SC}) including light harvesting efficiency and electron injection efficiency, have been discussed comprehensively. We hope this work will be helpful for the design of organic dyes with target properties to improve the performance of dye sensitized solar cells. All the dyes showed absorbance in visible region (502-521 nm) with high oscillator strength (f) (0.573-0.991) and light harvesting efficiency (LHE) (0.663-0.891). After binding to titanium oxide, all dye showed slightly red-shifted absorption (521-527 nm) with improved oscillator strength (f) (0.573-0.991) and light harvesting efficiency (LHE) (0.733-0.898). There is high probability that these dyes will show larger J_{SC} due to high driving force for electron injection. These dyes also showed larger V_{OC} (1.037-1.128 eV). The superior electron injection of dye 3 revealed that this heterocyclic azo dye might show better light to power conversion efficiency in DSSCs.

ACKNOWLEDGEMENT

Authors would like to acknowledge the support of the Ministry of Higher Education, Kingdom of Saudi Arabia for this research through a Grant (PCSED-006-14) under the Promising Centre for Sensors and Electronic Devices (PCSED) at Najran University, Kingdom of Saudi Arabia.

5. References

- [1] B. O'Regan, M. Gratzel, *Nature*, 353 (1991) 737-740.
- [2] S.-D. Khan, A. Mahmood, U. Rana, S. Haider, *Theor Chem Acc*, 134 (2014) 1-7.
- [3] A. Hagfeldt, M. Graetzel, *Chem. Rev.*, 95 (1995) 49-68.
- [4] J.N. Clifford, E. Martinez-Ferrero, A. Viterisi, E. Palomares, *Chemical Society Reviews*, 40 (2011) 1635-1646.
- [5] M.K. Nazeeruddin, F. De Angelis, S. Fantacci, A. Selloni, G. Viscardi, P. Liska, S. Ito, B. Takeru, M. Grätzel, *J. Am. Chem. Soc.*, 127 (2005) 16835-16847.
- [6] M.I. Abdullah, M.R.S.A. Janjua, M.F. Nazar, A. Mahmood, *Bulletin of the Chemical Society of Japan*, 86 (2013) 1272-1281.
- [7] T. Funaki, H. Funakoshi, O. Kitao, N. Onozawa-Komatsuzaki, K. Kasuga, K. Sayama, H. Sugihara, *Angewandte Chemie International Edition*, 51 (2012) 7528-7531.
- [8] A. Irfan, *Mater. Chem. Phys.*, 142 (2013) 238-247.
- [9] A. Irfan, A. Al-Sehemi, A. Asiri, *J. Mol. Model.*, 18 (2012) 3609-3615.
- [10] A. Irfan, A. Al-Sehemi, *J. Mol. Model.*, 18 (2012) 4893-4900.
- [11] S. Bagheri Novir, S.M. Hashemianzadeh, *Spectrochimica Acta A*, 143 (2015) 20-34.
- [12] A.G. Al-Sehemi, A. Irfan, A.M. Asiri, Y.A. Ammar, *J. Mol. Struct.*, 1019 (2012) 130-134.
- [13] A. Mishra, M.K.R. Fischer, P. Bäuerle, *Angew. Chem. Int. Ed.*, 48 (2009) 2474-2499.
- [14] A. Mahmood, S.U.-D. Khan, U.A. Rana, M.H. Tahir, *Arabian Journal of Chemistry*.
- [15] A. Mahmood, S.-D. Khan, U. Rana, *Journal of Computational Electronics*, 13 (2014) 1033-1041.
- [16] H.J. Snaith, *Advanced Functional Materials*, 20 (2010) 13-19.
- [17] M. Liang, J. Chen, *Chem. Soc. Rev.*, 42 (2013) 3453-3488.
- [18] B. Liu, W. Zhu, Q. Zhang, W. Wu, M. Xu, Z. Ning, Y. Xie, H. Tian, *Chemical Communications*, (2009) 1766-1768.
- [19] N. Martsinovich, A. Troisi, *Energy & Environmental Science*, 4 (2011) 4473-4495.
- [20] F. Borbone, A. Carella, L. Ricciotti, A. Tuzi, A. Roviello, A. Barsella, *Dyes and Pigments*, 88 (2011) 290-295.
- [21] J.A. Mikroyannidis, D.V. Tsagkournos, P. Balraju, G.D. Sharma, *Journal of Power Sources*, 196 (2011) 4152-4161.
- [22] T. Carofiglio, C. Fregonese, G.J. Mohr, F. Rastrelli, U. Tonellato, *Tetrahedron*, 62 (2006) 1502-1507.
- [23] M.M.M. Raposo, A.M.R.C. Sousa, A.M.C. Fonseca, G. Kirsch, *Tetrahedron*, 61 (2005) 8249-8256.
- [24] M.J. Frisch, G.W. Trucks, H.B. Schlegel, G.E. Scuseria, M.A. Robb, J.R. Cheeseman, G. Scalmani, V. Barone, B. Mennucci, G.A. Petersson, H. Nakatsuji, M. Caricato, X. Li, H.P. Hratchian, A.F. Izmaylov, J. Bloino, G. Zheng, J.L. Sonnenberg, M. Hada, M. Ehara, K. Toyota, R. Fukuda, J. Hasegawa, M. Ishida, T. Nakajima, Y. Honda, O. Kitao, H. Nakai, T. Vreven, J.A. Montgomery Jr., J.E. Peralta, F. Ogliaro, M.J. Bearpark, J. Heyd, E.N. Brothers, K.N. Kudin, V.N. Staroverov, R. Kobayashi, J. Normand, K. Raghavachari, A.P. Rendell, J.C. Burant, S.S.

- Iyengar, J. Tomasi, M. Cossi, N. Rega, N.J. Millam, M. Klene, J.E. Knox, J.B. Cross, V. Bakken, C. Adamo, J. Jaramillo, R. Gomperts, R.E. Stratmann, O. Yazyev, A.J. Austin, R. Cammi, C. Pomelli, J.W. Ochterski, R.L. Martin, K. Morokuma, V.G. Zakrzewski, G.A. Voth, P. Salvador, J.J. Dannenberg, S. Dapprich, A.D. Daniels, Ö. Farkas, J.B. Foresman, J.V. Ortiz, J. Cioslowski, D.J. Fox, Gaussian 09, in, Gaussian, Inc., Wallingford, CT, USA, 2009.
- [25] A.D. Becke, *The Journal of Chemical Physics*, 98 (1993) 5648-5652.
- [26] J. Zhang, H.-B. Li, S.-L. Sun, Y. Geng, Y. Wu, Z.-M. Su, *J. Mater. Chem.*, 22 (2012) 568-576.
- [27] J. Preat, C. Michaux, D. Jacquemin, E.A. Perpète, *The Journal of Physical Chemistry C*, 113 (2009) 16821-16833.
- [28] S. Kim, J.K. Lee, S.O. Kang, J. Ko, J.H. Yum, S. Fantacci, F. De Angelis, D. Di Censo, M.K. Nazeeruddin, M. Grätzel, *Journal of the American Chemical Society*, 128 (2006) 16701-16707.
- [29] D. Jacquemin, V. Wathelet, E.A. Perpète, C. Adamo, *Journal of Chemical Theory and Computation*, 5 (2009) 2420-2435.
- [30] M. Pastore, E. Mosconi, F. De Angelis, M. Grätzel, *The Journal of Physical Chemistry C*, 114 (2010) 7205-7212.
- [31] A. Saylam, Z. Seferoglu, N. Ertan, *Russ J Org Chem*, 44 (2008) 587-594.
- [32] T. Yanai, D.P. Tew, N.C. Handy, *Chem. Phys. Lett.*, 393 (2004) 51-57.
- [33] R. Kobayashi, R.D. Amos, *Chem. Phys. Lett.*, 420 (2006) 106-109.
- [34] I.S.K. Kerkines, I.D. Petsalakis, G. Theodorakopoulos, J. Rebek, *The Journal of Physical Chemistry A*, 115 (2011) 834-840.
- [35] I.V. Rostov, R.D. Amos, R. Kobayashi, G. Scalmani, M.J. Frisch, *The Journal of Physical Chemistry B*, 114 (2010) 5547-5555.
- [36] V. Barone, M. Cossi, *The Journal of Physical Chemistry A*, 102 (1998) 1995-2001.
- [37] P.J. Hay, W.R. Wadt, *The Journal of Chemical Physics*, 82 (1985) 270-283.
- [38] W.R. Wadt, P.J. Hay, *The Journal of Chemical Physics*, 82 (1985) 284-298.
- [39] P.J. Hay, W.R. Wadt, *The Journal of Chemical Physics*, 82 (1985) 299-310.
- [40] P. Qin, X. Yang, R. Chen, L. Sun, T. Marinado, T. Edvinsson, G. Boschloo, A. Hagfeldt, *The Journal of Physical Chemistry C*, 111 (2007) 1853-1860.
- [41] M. Gratzel, *Nature*, 414 (2001) 338-344.
- [42] G. Zhang, Y. Bai, R. Li, D. Shi, S. Wenger, S.M. Zakeeruddin, M. Gratzel, P. Wang, *Energy Environ. Sci.*, 2 (2009) 92-95.
- [43] H.S. Nalwa, *Handbook of Advanced Electronic and Photonic Materials and Devices*, Academic, San Diego, CA, 2001.
- [44] P. Persson, R. Bergström, L. Ojamäe, S. Lunell, Quantum-chemical studies of metal oxides for photoelectrochemical applications, in: *Advances in Quantum Chemistry*, Academic Press, 2002, pp. 203-263.
- [45] J. Preat, D. Jacquemin, C. Michaux, E.A. Perpète, *Chemical Physics*, 376 (2010) 56-68.
- [46] R.G. Pearson, *Inorg. Chem.*, 27 (1988) 734-740.
- [47] C.-R. Zhang, Z.-J. Liu, Y.-H. Chen, H.-S. Chen, Y.-Z. Wu, W. Feng, D.-B. Wang, *Current Applied Physics*, 10 (2010) 77-83.

Tables

Table 1. Functional and basis set effect on λ_{\max} of reference dye.

Basis Set	B3LYP	CAM-B3LYP
6-31G	405	412
6-31+G	422	430
6-31+G*	430	436
6-31+G**	456	452

The experimental value is 442 nm[31].

Table 2. Computed maximum absorption wavelengths (λ_{\max} / nm), absorption energy (E_g / eV), oscillator strengths (f), light harvesting efficiency (LHE) and transition natures of dyes.

Dye	λ_{\max}	E_g	f	LHE	Main configurations
1	521.73	2.023	0.764	0.828	H \rightarrow L (87%)
2	516.67	2.151	0.473	0.663	H \rightarrow L (65%)
3	502.34	2.341	0.961	0.891	H-1 \rightarrow L (74%)
4	507.23	2.340	0.923	0.881	H \rightarrow L (63%)

H stands for HOMO and L stands for LUMO

Table 3. Computed maximum absorption wavelengths (λ_{\max} / nm), absorption energy (E_g / eV), oscillator strengths (f), light harvesting efficiency (LHE) and transition natures of dyes@TiO₂cluster.

Dye	λ_{\max}	E_g	f	LHE	Main configurations
1	527.16	1.960	0.844	0.857	H-2 \rightarrow L+13 (77%)
2	523.19	2.024	0.573	0.733	H-3 \rightarrow L+8 (69%)
3	522.77	2.014	0.991	0.898	H-2 \rightarrow L+10 (64%)
4	521.66	2.113	0.970	0.893	H-1 \rightarrow L+11 (55%)

H stands for HOMO and L stands for LUMO

Table 4. ΔG^{inject} (eV), oxidation potential (eV) and V_{oc} (eV) of dyes.

Dye	ΔG^{inject}	E_{ox}^{dye*}	E_{ox}^{dye}	V_{oc}
1	-0.103	3.897	5.920	1.128
2	-0.191	3.809	5.960	1.068
3	-0.237	3.763	6.104	1.037
4	-0.136	3.864	6.204	1.046

Figures

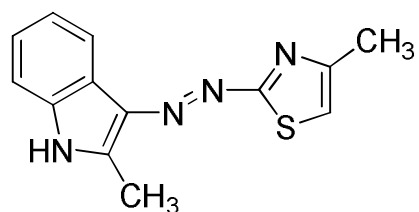


Fig. 1: Structure of reference dye

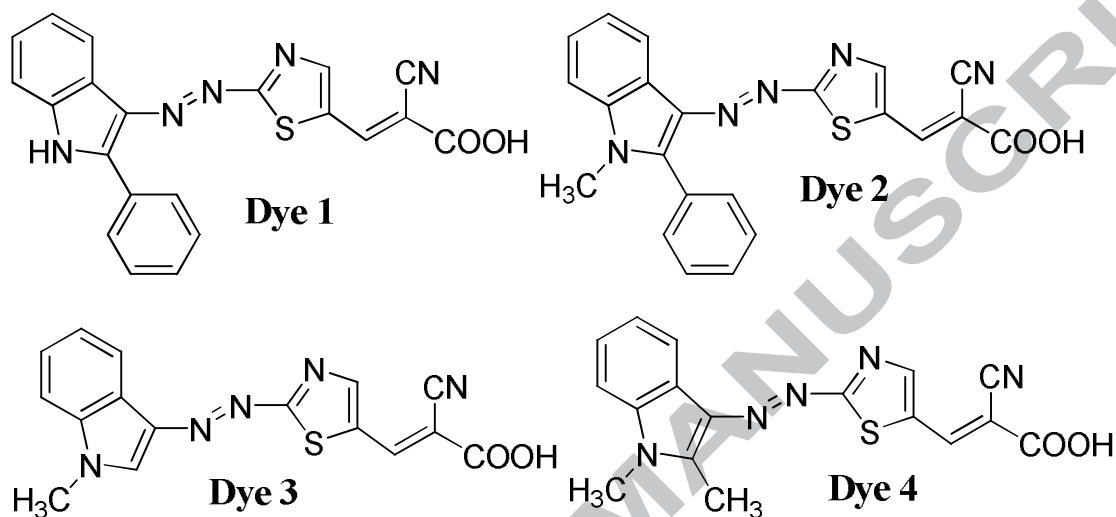
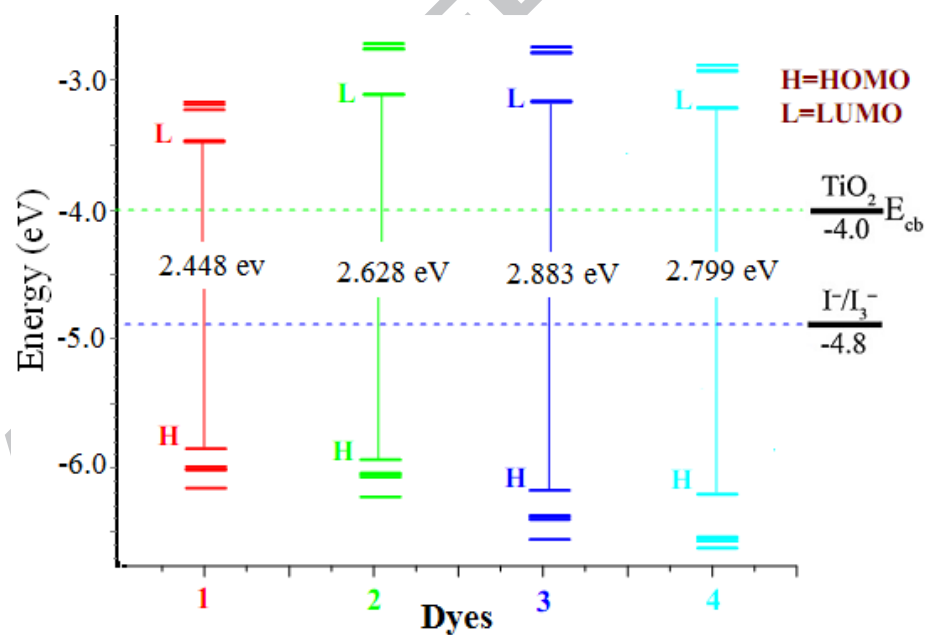


Fig. 2: Structures of designed dyes

Fig. 3: Schematic energy diagram of dyes, TiO_2 and electrolyte (I^-/I_3^-), E_{HOMO} and E_{LUMO} of the dyes.

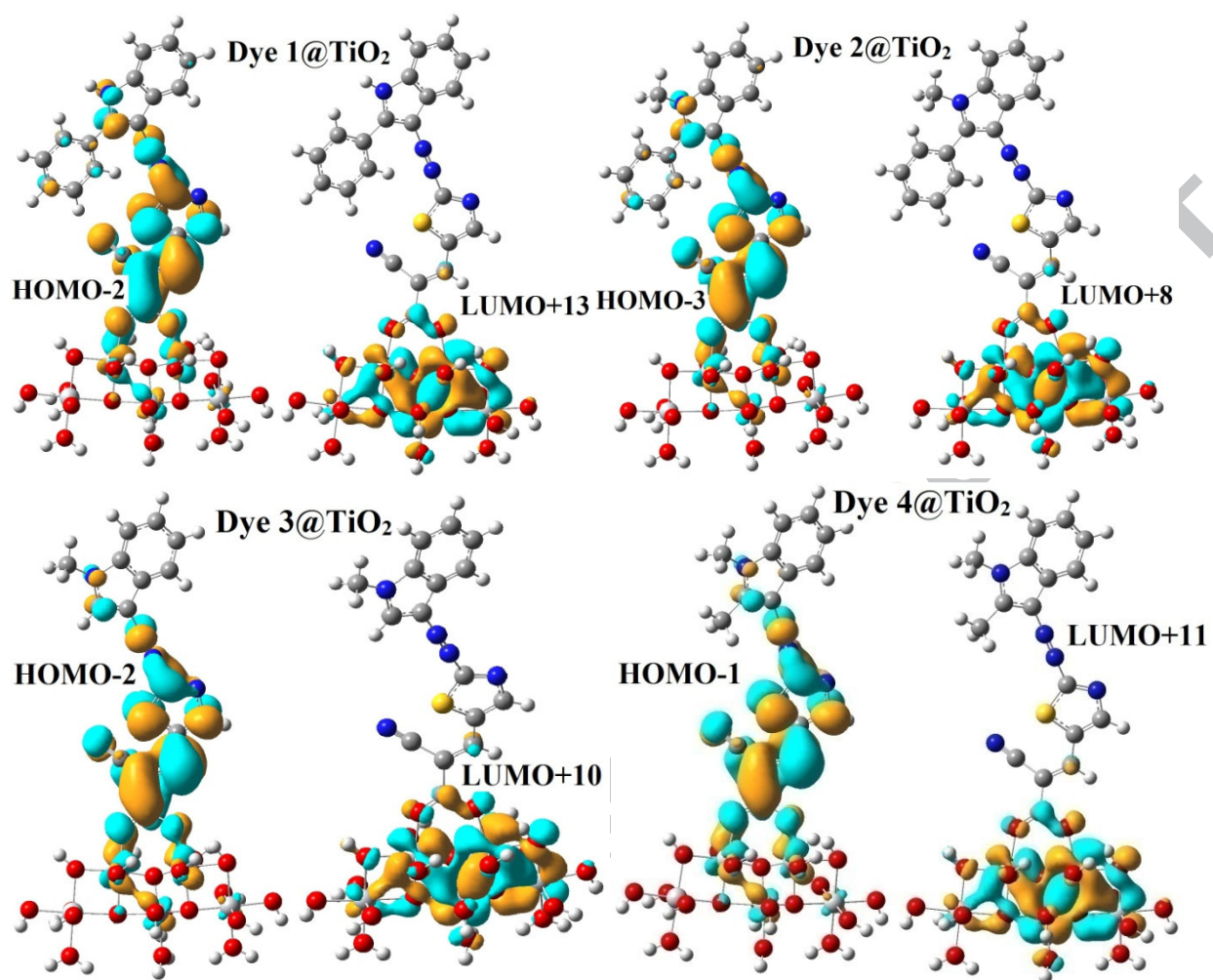
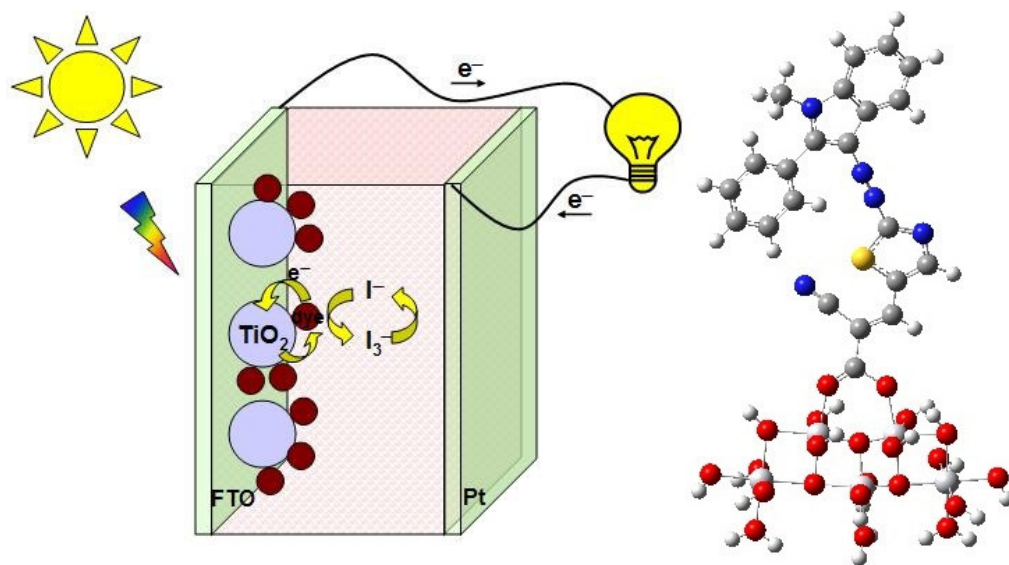


Fig. 4: HOMO and LUMO of studied dyes@TiO₂ cluster.

Graphical Abstract



Highlights

1. New small size heterocyclic azo dyes were theoretically designed.
2. DFT and TD-DFT calculations were performed.
3. Absorption spectra of the dyes were simulated.
4. V_{OC} , LHE and the electron injection efficiency were calculated approximately.
5. These dyes are expected to show better light to power conversion efficiency in DSSCs.